Acta Med. Okayama, 2018
Vol. 72, No. 1, pp. 53–59

Acta Medica Okayama
http://escholarship.lib.okayama-u.ac.jp/amo/

Original Article

The Usefulness of Readout-Segmented Echo-Planar Imaging (RESOLVE) for Bio-phantom Imaging Using 3-Tesla Clinical MRI

Yuuki Yoshimura[a,b], Masahiro Kuroda[a]*, Irfan Sugianto[c], Babatunde O. Bamgbose[c], Kanae Miyahara[a,b], Yuichi Ohmura[a], Akira Kurozumi[a,d], Toshi Matsushita[d], Seiichiro Ohno[d], Susumu Kanazawa[e], and Junichi Asaumi[c]

[a]Radiological Technology, Graduate School of Health Sciences, Okayama University, Departments of [c]Oral and Maxillofacial Radiology and [e]Radiology, Okayama University Graduate School of Medicine, Dentistry and Pharmaceutical Sciences, [d]Central Division of Radiology, Okayama University Hospital, Okayama 700-8558, Japan, [b]Radiology Diagnosis, Okayama Saiseikai General Hospital, Okayama 700-8511, Japan

Readout-segmented echo-planar imaging (RESOLVE) is a multi-shot echo-planar imaging (EPI) modality with k-space segmented in the readout direction. We investigated whether RESOLVE decreases the distortion and artifact in the phase direction and increases the signal-to-noise ratio (SNR) in phantoms image taken with 3-tesla (3T) MRI *versus* conventional EPI. We used a physiological saline phantom and subtraction mapping and observed that RESOLVE's SNR was higher than EPI's. Using RESOLVE, the combination of a special-purpose coil and a large-loop coil had a higher SNR compared to using only a head/neck coil. RESOLVE's image distortion was less than EPI's. We used a 120 mM polyethylene glycol phantom to examine the phase direction artifact. The range where the artifact appeared in the apparent diffusion coefficient (ADC) image was shorter with RESOLVE compared to EPI. We used RESOLVE to take images of a Jurkat cell bio-phantom: the cell-region ADC was 856×10^{-6} mm^2/sec and the surrounding physiological saline-region ADC was $2{,}951 \times 10^{-6}$ mm^2/sec. The combination of RESOLVE and the 3T clinical MRI device reduced image distortion and improved SNR and the identification of accurate ADC values due to the phase direction artifact reduction. This combination is useful for obtaining accurate ADC values of bio-phantoms.

Key words: RESOLVE, bio-phantom, 3 tesla MRI, apparent diffusion coefficient, diffusion-weighted imaging

Diffusion-weighted imaging (DWI) magnetic resonance imaging (MRI) is useful for the early diagnosis of cerebrovascular disorders such as cerebral infarction and tumors. In imaging used for tumor diagnoses, the apparent diffusion coefficient (ADC) is routinely obtained to determine whether the lesion is benign or malignant and to predict the patient's therapeutic response [1], but the mechanism(s) underlying the decrease of an ADC value in tumors are not known. For the elucidation of these mechanisms, it is necessary to observe the diffusion phenomena at the basic experimental level, using bio-phantoms and clinical MRI equipment.

In a previous study, we succeeded in imaging cells using a bio-phantom and 1.5 tesla (T) clinical MRI [2]. The use of 3T MRI devices in daily clinical practice has become more common. The signal-to-noise ratio (SNR) of 3T MRI is twice that of 1.5T MRI, and 3T images have higher resolution. The 3T imaging time is also

Received May 18, 2017; accepted September 22, 2017.
*Corresponding author. Phone: +81-86-235-6873; Fax: +81-86-235-6873
E-mail: kurodamd@cc.okayama-u.ac.jp (M. Kuroda)

Conflict of Interest Disclosures: No potential conflict of interest relevant to this article was reported.

shorter. The doubling of the chemical shift in 3T imaging is advantageous for MR spectroscopy, and the effect of fat suppression also increases. As the susceptibility effect doubles, the uniformity of the magnetic field increases. Based on these characteristics, in our previous unpublished study using a bio-phantom and a clinical 3T MRI system with echo-planar imaging (EPI), it was difficult to accurately measure the ADC value due to phase direction artifacts, including N/2 (N-Half) artifacts. The N/2 artifact is unique to the EPI method, in which phase errors may result from the multiple positive and negative passes through k-space [3]. This disadvantage of EPI is caused by various uncertain factors such as an eddy current due to magnetic field inhomogeneity, instrument instability, an incomplete gradient magnetic field, and other factors [3].

Readout-segmented echo-planar imaging (EPI), known as RESOLVE (REadout Segmentation Of Long Variable Echo-trains) [4,5], was introduced in clinical studies as one of the DWI methods so that distortion in the phase direction can be reduced. Here we thus examined whether RESOLVE is effective for reducing the artifact in the phase direction including N/2 artifact. We investigated the usefulness of RESOLVE compared to EPI in bio-phantom imaging using a clinical 3T MRI device. We evaluated the distortion, SNR, phase-direction artifact, and bio-phantom images.

Materials and Methods

Liquid phantoms and bio-phantom. For a liquid phantom, we put physiological saline (0.9% NaCl) in a micro-cuvette (Halb-Mikro 1.5 ml, Greiner, Düsseldorf, Germany) and placed the micro-cuvette in a plastic container (external dia. 9.5 cm, width 14 cm, height 7 cm). As another liquid phantom, we put 120 mM polyethylene glycol (PEG) [6] in a micro-cuvette (Halb-Mikro 1.5 ml, Greiner). As the bio-phantom [7], we used Jurkat cells purchased from RIKEN Cell Bank (Ibaraki, Japan). For culturing, 10% fetal bovine serum (Filtron, Victoria, Australia) and 1% penicillin-streptomycin-neomycin (Gibco, Grand Island, NY, USA) were added to RPMI 1640 medium (pH 7.4; Gibco). The incubation was carried out at 37°C with 5% CO_2. When a spinner flask (#3153, Corning, New York, NY, USA) was used for a culture, a rotary incubator was use at 15 rpm (ULS-4, As One, Tokyo, Japan). We counted the number of cells with a dia. >8 μm with an electric cell counter (Coulter Electronics, Luton, UK) before the bio-phantom preparation, because the dia. of most of the Jurkat cells was >8 μm, with the average dia. being 9.6 μm.

The Jurkat cells were encapsulated into bio-phantoms as described [7]. Briefly, after measuring the cell number, we concentrated the cell solution to approx. 2 ml, placed it in a micro-cuvette (Halb-Mikro 1.5 ml, Greiner), centrifuged the solution at 1200 rpm for 5 min, removed the supernatant and adjusted the cell density to 6.78×10^8 cells/ml. After treatment, the cells were enclosed in gellan gum (P-8169; Sigma Chemicals, St. Louis, MO, USA).

MRI system. A 3T MRI system (Magnetom Skyra, Siemens Healthcare, Erlangen, Germany) was used. Its coils are a four-channel 'special-purpose coil,' an 11-cm 'large-loop coil,' and a 20-channel 'head/neck coil.'

Measurement of the SNR. We investigated the SNR with the use of different sequences and coils. Physiological saline was used as the phantom. For the SNR examination using different sequences, the special-purpose coil was placed below the phantom and the large-loop coil was placed on top of the phantom. Both the RESOLVE and EPI images were taken at room temperature. In the measurement of SNR using the three different coils, RESOLVE images were taken at room temperature with the head/neck coil and with the combination of the special-purpose coil and the large-loop coil.

We used the subtraction mapping method [8] for the SNR analysis, as this method can evaluate the SNR in a sequence using parallel imaging (including RESOLVE). More specifically, the phantom was imaged twice under the same conditions, and a subtraction image was created. The SNR was obtained by dividing the signal average value in the range of approx. 7×7 pixels of one of the images captured twice by the standard deviation in the same region of the subtraction image and multiplied by the square root of 2 ($\sqrt{2}$). These calculations were performed for each pixel to calculate and create an SNR map. The region of interest (ROI) was set to include >75% of the phantom area on this SNR map, and the SNR was defined as the average value in the ROI.

Evaluation of distortion. The phantom for the evaluation of distortion was the physiologic saline-filled plastic container described above. We examined whether the content of the micro-cuvette, *i.e.*, air or physiologic

saline, affected the distortion. The special-purpose coil was placed below the phantom, and the large-loop coil was placed on top of the phantom. Both the RESOLVE and EPI images were taken at room temperature. The T2-weighted images were also taken, as reference images without distortion. The images were taken when the micro-cuvette was filled with physiological saline and when the amount of physiological saline in the micro-cuvette was gradually decreased and the air layer increased. The extent of distortion on the images was evaluated visually.

Evaluation of the phase-direction artifact. The phantom for our evaluation of the phase-direction artifact was composed of 120 mM PEG in a micro-cuvette. The micro-cuvette was placed in a physiologic saline-filled plastic container. The container was placed in a heating device that we constructed (made of ethylene-vinyl acetate copolymer) and connected to a circulation thermostatic chamber (Thermo-Mate BF-41, Yamato Scientific Co., Tokyo, Japan). For the real-time phantom temperature measurements, an optical fiber thermometer (Fluoroptic® m3300 series thermometer, Luxtron Co., Santa Clara, CA, USA) was installed 5 mm above the bottom of the micro-cuvette, and during the MR imaging. the special-purpose coil was placed under the heating device, and large-loop coil was placed on top of the heating device. RESOLVE and EPI images were taken while the phantom was warmed to 37°C.

Since the phase direction of this setting was the longitudinal axis of the micro-cuvette, a profile of the signal intensity was taken from each pixel of the RESOLVE and EPI images along the midline of the longitudinal axis (from the bottom to the top) of the micro-cuvette. The natural logarithm value of each signal intensity was calculated. The *b*-values between 0 and 1,300 sec/mm^2 were plotted on the horizontal axis, and the natural logarithm signal for each *b*-value was plotted on the vertical axis. We calculated used the least-square method to calculate the slope, and the ADC values are represented as the negative values of the slope. ADC values were plotted on the longitudinal axis as a function of the b-value on the horizontal axis, from the bottom to the top of the micro-cuvette. The range of the phase-direction artifact of the ADC values along the longitudinal axis was evaluated.

Evaluation of the bio-phantom. The bio-phantom was Jurkat cells encapsulated in a micro-cuvette placed in a physiologic saline-filled plastic container. The container was placed in a self-made heating device connected to a circulation thermostatic chamber (Thermo-Mate BF-41). For the real-time phantom temperature measurements, an optical fiber thermometer (Fluoroptic ™ thermometer m3300) was installed 5 mm above the bottom of the micro-cuvette during the MR imaging. The special-purpose coil was placed under the heating device, and the large-loop coil was placed on top of the heating device. RESOLVE images were taken while the phantom was warmed to 37°C. The signal intensities of the ROI of 6×6 pixels at 5 mm above the bottom of the bio-phantom and that of the physiological saline at the same height were measured for each *b*-value between 0 and 2,000 sec/mm^2. Using these signal intensities, we calculated the ADC values of the bio-phantom and physiological saline.

MR imaging method. RESOLVE and EPI images were taken for the evaluations of the SNR, distortion, phase-direction artifact, and bio-phantom. The MR imaging conditions used are summarized in Table 1.

MR image analysis. MR images were transferred into and analyzed using the image analysis software, ImageJ ver. 1.51 g (U.S. National Institutes of Health, Bethesda, MD).

Results

The SNR

1. The difference in SNR by RESOLVE vs. EPI sequence

The use of RESOLVE improved the SNR, as shown in Fig. 1A, B. The SNR values were 46.2 and 21.7 for RESOLVE and EPI, respectively.

2. The difference in the SNR due to the selection of coils

The combination of the special-purpose coil and large-loop coil improved the SNR (Fig. 1A, C). The SNR value was 46.2 for the combination of the special-purpose coil and large-loop coil, and 23.5 for the head/neck coil.

Distortion of images

1. The difference in distortion by sequence

RESOLVE (Fig. 2B, E) lessened the distortion compared to EPI (Fig. 2C, F) despite the air in the phantom.

2. The difference in distortion by the amount of air in the phantom

With both RESOLVE (Fig. 2B, E) and EPI (Fig. 2C, F),

Table 1 RESOLVE and EPI MR imaging conditions, SNR, distortion, phase-direction artifact and bio-phantom

Parameters	SNR and distortion		Phase direction artifact		Bio-phantom
	RESOLVE	EPI	RESOLVE	EPI	RESOLVE
TR (msec)	8000	8000	8000	8000	8000
TE (msec)	80	122	103	98	103
ES (msec)	0.6	1.57	0.6	1.44	0.6
FOV (mm)	120	120	120	120	120
Matrix	162 × 162	162 × 162	224 × 224	120 × 120	224 × 224
BW (Hz/pixel)	386	752	360	758	360
Average	2	2	2	2	2
Segment	7	–	7	–	7
Slice thickness (mm)	5	5	5	5	5
Slice number	1	1	1	1	1
Phase direction	AP	AP	AP	AP	AP
b-value (sec/mm^2)	1000	1000	0, 200, 400, 600, 800, 1000, 1100, 1200, 1300	0, 200, 400, 600, 800, 1000, 1100, 1200, 1300	0, 200, 400, 600, 800, 1000, 1100, 1200, 1300, 1400, 1500, 1700, 2000
Imaging time (h : min : sec)	7 : 06	1 : 14	1 : 43 : 30	12 : 42	1 : 43 : 30

TR, repetition time; TE, echo time; ES, echo space; FOV, field of view; BW, band width; AP, antero-posterior.

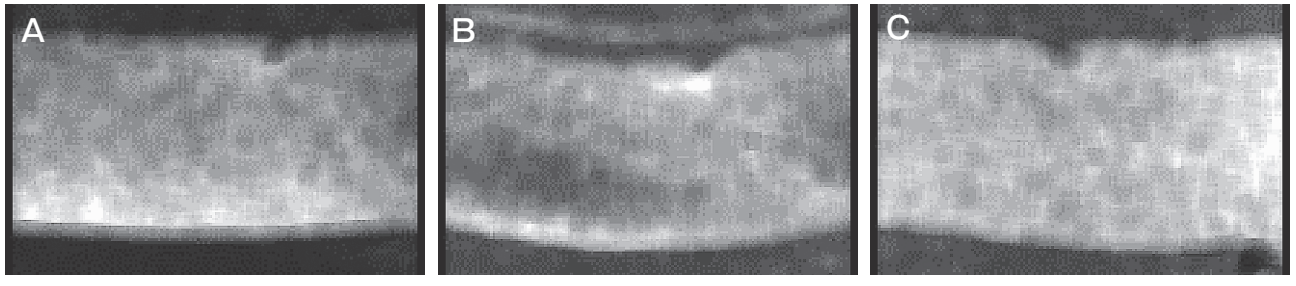

Fig. 1 The SNR map based on the differences in sequences and in the selection of coils. **A**, RESOLVE with the combination of the special-purpose coil and large-loop coil. SNR: 46.2; **B**, EPI with the combination of the special-purpose coil and large-loop coil. The SNR was 21.7; **C**, RESOLVE with the head/neck coil. SNR: 23.5.

the degree of distortion increased as the air volume in the phantom increased.

Phase-direction artifact. The RESOLVE (Fig. 3B) and EPI (Fig. 3C) images were taken for the phantom containing 120 mM PEG (Fig. 3A). The phase-direction artifact appeared at the bottom of the phantom in both sequences (Fig. 3D). However, the range of the artifact of RESOLVE (4.82 mm) was narrower than that of EPI (11.00 mm).

Evaluation of bio-phantom. Fig. 4 illustrates the calculation of the ADC values of the bio-phantom. The signal intensity of the ROIs on each RESOLVE image was plotted as a function of the *b*-values. The regression lines were made for the bio-phantom and the physiological saline using the least-squares method for the *b*-values between 0 and 1,300 sec/mm^2. Within this range of *b*-values, the R^2 in regression was >0.99. The ADC values were calculated as the negative value of these slopes. The ADC values were 856×10^{-6} mm^2/sec for the bio-phantom and $2{,}951 \times 10^{-6}$ mm^2/sec for the physiological saline.

Discussion

We examined the possibility of cell imaging using a clinical 3T MRI system with RESOLVE. Our findings confirmed the improvement of the SNR and the lessening of distortion in addition to an improvement of the

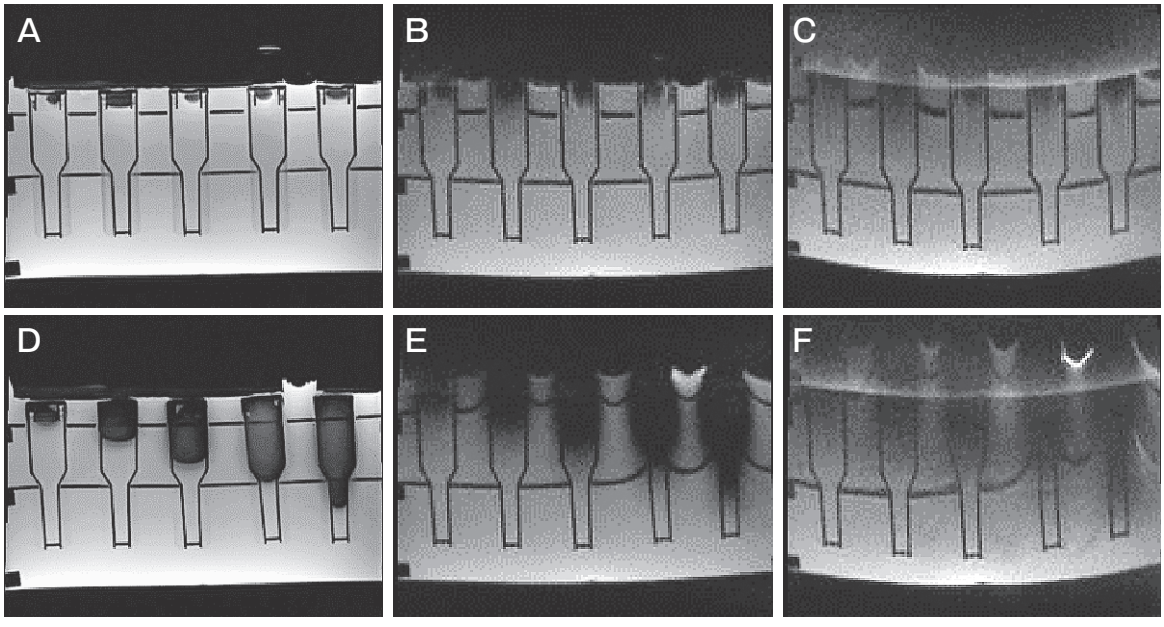

Fig. 2 The distortion of images based on the different sequences and the volume of air in the phantom. **A**, **D**, T2-weighted images as the control images without distortion; **B**, **E**, RESOLVE; **C**, **F**, EPI. **A**–**C**, No air in the phantom; **D**–**F**, Different volumes of air in the phantom.

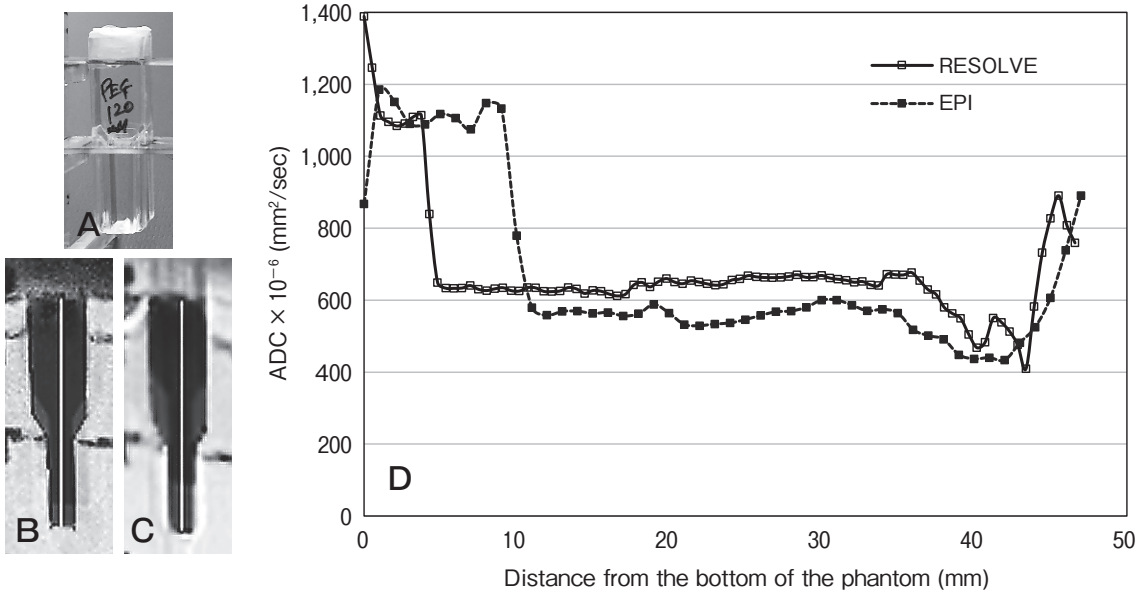

Fig. 3 The phase-direction artifact. **A**, The phantom containing 120 mM PEG; **B**, RESOLVE; **C**, EPI. The longitudinal axis of the phantom represents the phase direction; this is shown as the midline on panels B and C; **D**, The ADC values calculated along the midline of the longitudinal axis, from the bottom to the top of the phantom. Open square with full line, RESOLVE; Closed square with dotted line, EPI.

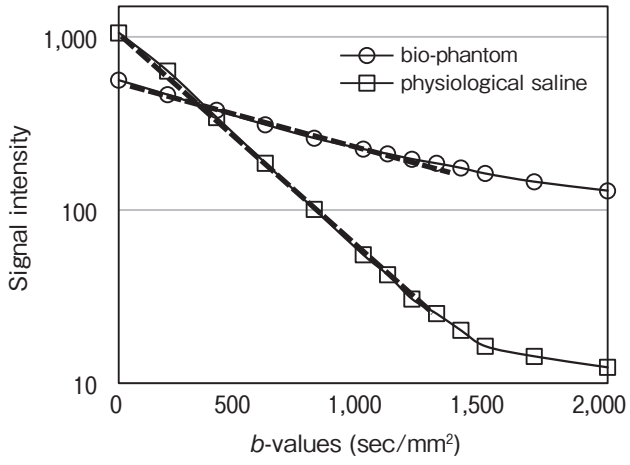

Fig. 4 Calculation of the ADC values of the bio-phantom. The signal intensity of the ROIs on the RESOLVE images was plotted as the function of the *b*-values. Open circles and squares represent the signal intensity of the ROIs in the bio-phantom and physiological saline, respectively. The straight lines represent regression lines calculated with the least square method for the *b*-values between 0 and 1,300 sec/mm^2.

accuracy of ADC value measurement due to a reduction of the phase-direction artifact by RESOLVE.

Clinical 3T MRI compared to conventional 1.5T MRI has the advantage of high signal intensity and a high SNR that improve the image quality. On the other hand, clinical 3T MRI has the disadvantages of increased susceptibility effect and magnetic field non-uniformity, which cause an increases in the dephasing and the distortion of the images. RESOLVE—one of the DWI techniques which decrease the dephasing and can reduce distortion—was introduced into clinical studies around the year 2008 to overcome these disadvantages [4,5]. With EPI, a conventional DWI technique, the single excitation fills the echo signals into the entire k-space. During this period of echo filling, dephasing progresses and causes distortion of the image.

RESOLVE is a new multi-shot EPI approach in which the k-space is divided into multiple segments in the readout direction, compared to EPI, With RESOLVE, the excitation repeats for each segment. The echo signals are filled one-by-one into each segment and, as the period of signal filling of each segment is short compared to EPI, dephasing cannot develop during each period. As a result, the total dephasing becomes small compared to EPI, resulting in the reduction of the distortion of images [5].

Our present findings clarify that RESOLVE improves the SNR. Multi-shot EPI has been reported to improve the SNR [9]. The SNR improvement might be explained by the higher signal intensity (because of small dephasing) of RESOLVE compared to EPI. When DW images are taken with a short effective TE, the signal intensity increases due to the short echo space [10]. As the k-space is segmented with RESOLVE and the effective TE is shortened, this might account for the improved SNR.

The phase-direction artifacts, including N/2 artifacts, are decreased with RESOLVE, probably due to the decrease of the influence of magnetic field inhomogeneity with short TE imaging.

We measured the ADC value of the bio-phantom using RESOLVE at 37°C, which is equivalent to the human body's temperature. The ADC value of the physiological saline at that temperature was $2{,}951 \times 10^{-6}$ mm^2/sec, which was almost the same as the theoretical diffusion of water, $3{,}000 \times 10^{-6}$ mm^2/sec, at 37°C.

The usefulness of RESOLVE with clinical 3T MRI has been reported in the diagnosis of breast cancer and prostate cancer [11,12]. The results of our present study indicate that RESOLVE improves the accuracy of ADC value measurement due to the decrease in the phase-direction artifact, suggesting that the application of RESOLVE in clinical 3T MRI may lead to a more accurate diagnosis of tumors.

The imaging time of RESOLVE (*i.e.*, within the range between 7 min 6 sec and 1 h 43 min 30 sec) was longer than that of EPI (within the range between 1 min 14 sec and 12 min 42 sec). The imaging time of RESOLVE was long in the present bio-phantom investigation because multiple *b*-values were used for the imaging. The imaging time of RESOLVE in clinical use is usually short, such as 3 min, with a few *b*-values. We used the combination of a special-purpose coil and a large-loop coil for the imaging of the bio-phantom because this combination was superior to the head/neck coil for the imaging of a small object. However, the selection of a coil usually depends on the size of the objects in clinical use.

In conclusion, RESOLVE with clinical 3T MRI is useful for the reduction of image distortion, improved SNR, and the accurate measurement of ADC values due to the reduced phase-direction artifact. The accurate ADC value measurement of the present bio-phantom was possible with RESOLVE and clinical 3T MRI.

Acknowledgments. We thank the staff of the Department of Radiology and the Central Division of Radiology of Okayama University Hospital for their support. This study was partially supported by a Grant-in-Aid for Scientific Research [C (15K09924)] from the Ministry of Health, Labour and Welfare of Japan.

References

1. Shinmoto H and Oshio K: High b-value diffusion-weighted MR imaging. Jpn J Magn Reson Med (2008) 28: 114–121 (in Japanese).
2. Matsumoto Y, Kuroda M, Matsuya R, Kato H, Shibuya K, Oita M, Kawabe A, Matsuzaki H, Asaumi J, Murakami J, Katashima K, Ashida M, Sasaki T, Sei T, Kanazawa S, Mimura S, Oono S, Kitayama T, Tahara S and Inamura K: *In vitro* experimental study of the relationship between the apparent diffusion coefficient and changes in cellularity and cell morphology. Oncol Rep (2009) 22: 641–648.
3. Hashemi RH, Bradley Jr. WG and Lisanti CJ: Gradient echo: part II (fast scanning techniques); in MRI the basics, 3rd Ed, Lippincott Williams & Wilkins (2010) pp 261.
4. Holdsworth SJ, Skare S, Newbould RD, Guzmann R, Blevins NH and Bammer R: Readout-segmented EPI for rapid high resolution diffusion imaging at 3T. Eur J Radiol (2008) 65: 36–46.
5. Porter DA and Heidemann RM: High resolution diffusion-weighted imaging using Readout-segmented echo-planar imaging, Parallel imaging and a two-dimensional navigator-based reacquisition. Magn Reson Med (2009) 62: 468–475.
6. Matsuya R, Kuroda M, Matsumoto Y, Kato H, Matsuzaki H, Asaumi J, Murakami J, Katashima K, Ashida M, Sasaki T, Sei T, Himei K, Katsui K, Katayama N, Takemoto M, Kanazawa S, Mimura S, Oono S, Kitayama T, Tahara S and Inamura K: A new phantom using polyethylene glycol as an apparent diffusion coefficient standard for MR imaging. Int J Oncol (2009) 35: 893–900.
7. Katashima k, Kuroda M, Ashida M, Sasaki T, Taguchi T, Matsuzaki H, Murakami J, Yanagi Y, Hisatomi M, Hara M, Kato H, Ohmura Y, Kobayashi T, Kanazawa S, Harada S, Takemoto M, Ohno S, Mimura S and Asaumi J: *In vitro* assessment of factors affecting the apparent diffusion coefficient of Jurkat cells using bio-phantoms. Acta Med Okayama (2013) 67: 359–367.
8. Imai H, Miyati T, Ogura A, Doi T, Tsuchihashi T, Machida Y, Kobayashi M, Shimizu K and Kitou Y: Signal-to-noise ratio measurement in parallel MRI with subtraction mapping and consecutive methods. Jpn J Radiol Technol (2008) 64: 930–936 (in Japanese).
9. Val MR, Wolfgang RN, Miguel T and Frank LG: Advanced image acquisition strategies; in The physics of clinical MR taught through images, Oshio K and Momoshima S eds, 1st Ed, Medical Sciences International Ltd (2015) pp 126–127 (in Japanese).
10. Ohno N: Diffusion analysis; in MRI evaluation and analysis, Miyati T ed, 1st Ed, Ohmsha Ltd (2012) pp 182–184 (in Japanese).
11. Li L, Wang L, Deng M, Liu H, Cai J, Sah VK and Liu J: Feasibility study of 3-T DWI of the prostate: Readout-segmented versus single-shot echo-planar imaging. Am J Roentgenol (2015) 205: 70–76.
12. Filli L, Ghafoor S, Kenkel D, Liu W, Weiland E, Andreisek G, Frauenfelder T, Runge VM and Boss A: Simultaneous multi-slice readout-segmented echo planar imaging for accelerated diffusion-weighted imaging of the breast. Eur J Radiol (2016) 85: 274–278.